RESEARCH ARTICLE
doi: 10.2306/scienceasia1513-1874.2024.040

ScienceAsia 50 (2): 2024: ID 2024040: **1–11**

Characteristics of rare earth minerals in greisen and skarn Sn deposits at Ban Khao area, Kanchanaburi Province, Thailand

Bussayawan Sukbunjong[a], **Ladda Tangwattananukul**[a,*]

[a] Department of Earth Sciences, Faculty of Science, Kasetsart University, Bangkok 10900 Thailand

[*]Corresponding author, e-mail: fscildt@ku.ac.th

Received 7 Jul 2023, Accepted 27 Dec 2023
Available online 3 May 2024

ABSTRACT: Rare earth mineralization in Thailand occurs related to Sn deposits in many provinces including Kanchanaburi, Ranong, and Phuket. Kanchanaburi is one of the large Sn mineralization provinces, which contains the Jarin Sn mine in Ban Khao. The geology of the Ban Khao area comprises limestone, sandstone, and mudstone from Ordovician to Permian, intruded by Cretaceous granites, which are associated with greisenization and skarn Sn deposits. This paper clarifies the hydrothermal alterations related to the rare earth element (REE) mineralization in the greisen and skarn at the Ban Khao area, Kanchanaburi Province based on their rare earth mineral characteristics, mineral assemblages in the veins, and the hydrothermal alteration of granite and skarn. The geology of the Huai Heang area comprises tourmaline-biotite granite and aplite. These rocks are associated with the quartz-zinnwaldite-muscovite-cassiterite-tourmaline and quartz veins which contain greisenization Sn deposits. Monazite and xenotime are present as accessory minerals in the tourmaline-biotite granite and aplite in the Huai Heang and Khao Phu I Kang areas. In contrast, thorite, euxenite, columbite, and britholite occur in the strongly altered tourmaline-biotite granite and the quartz-zinnwaldite-muscovite-cassiterite-tourmaline vein of greisen Sn deposit in the Huai Heang area. Monazite contains high concentrations of light rare earth elements (LREEs) (Ce_2O_3, La_2O_3, and Nd_2O_3). Xenotime contains heavy rare earth elements (HREEs) (Y_2O_3, Gd_2O_3, and Dy_2O_3). Thorite, euxenite, and columbite are major HREE minerals, whereas britholite, occurring in fractures of apatite, contains both LREEs and HREEs. These rare earth minerals were formed by hydrothermal activities that caused greisenization and Sn mineralization in the strongly altered tourmaline-biotite granite.

KEYWORDS: monazite, greisenization, hydrothermal REE mineral deposit, Ban Khao Sn deposit

INTRODUCTION

Rare earth elements (REEs) have been in demand since 1990 as essential parts of many high-tech devices, especially in the field of communication tools and equipment such as computers and mobile phones which contain rare earth magnets [1, 2]. China is a leading producer of REEs [1, 2]. Due to the limited exportation of REEs from China in 2010, other countries started exploring their own REE resources. Most global REE deposits are associated with carbonatite, alkaline granite, Fe-REEs deposits, hydrothermal deposits, marine placer, alluvial placer, and ion-adsorption type [2, 3].

Thailand contains the Eastern, Central, and Western Granite Belts. The Western Granite Belt is mainly composed of alkaline granite (S-type granite) (Fig. 1(a)) [4–6]. The alkaline granite is associated with tin (Sn) and tungsten (W) deposits and contains REE occurrences in Chaing Rai, Mae Hong Son, Kanchanaburi, Ranong, Phang Nga, and Phuket Provinces, as shown in Fig. 1(a) [6–8]. Large Sn deposits in Kanchanaburi Province are in Thong Pha Phum (Pilok mine, Pilok area), Sai Yok (Bong Ti mine, Bong Ti area), and Muang District (Jarin mine, Ban Khao area). These Sn deposits are hosted in porphyritic biotite granite, tourmaline-muscovite granite, and biotite-muscovite granite of Cretaceous [9–11]. The Sn, W, and REE mineralization is associated with greisenization and skarn represented by the Pilok greisen Sn deposit and the Pin Yok skarn Sn deposit [10, 11]. The greisen mineral assemblage in the Sn deposits is composed of quartz, muscovite, topaz, tourmaline, and fluorite with monazite, zircon, and apatite [12, 13], while the skarn Sn deposit is associated with quartz, calcite, pyroxene, garnet, vesuvianite, wollastonite, and epidote [14, 15].

The Ban Khao study area, Muang District, Kanchanaburi Province, is a large Sn production area. The Jarin Sn deposit produced approximately 5,400 tons of Sn concentration at 900 g/m^3 Sn from 1975 to 1984 [9]. The Sn deposits in the Ban Khao area contain greisen Sn deposit (Jarin) and Skarn Sn deposit which are related to alkaline granite and hydrothermal deposit. This research clarifies the hydrothermal alterations related to REE mineralization in the greisen and skarn in the Ban Khao area, Kanchanaburi Province based on their rare earth mineral characteristics, mineral assemblages in the veins, and hydrothermal alteration of the granite and skarn.

GEOLOGY OF THE STUDY AREA

Granite in Southeast Asia extends from Myanmar across Thailand to Peninsular Malaysia and is separated into the Eastern (220–263 Ma), Central (207–237 Ma), and Western Granite Belt (22–149 Ma) (Fig. 1(a)) [4–6, 16, 17]. The Eastern Granite Belt was

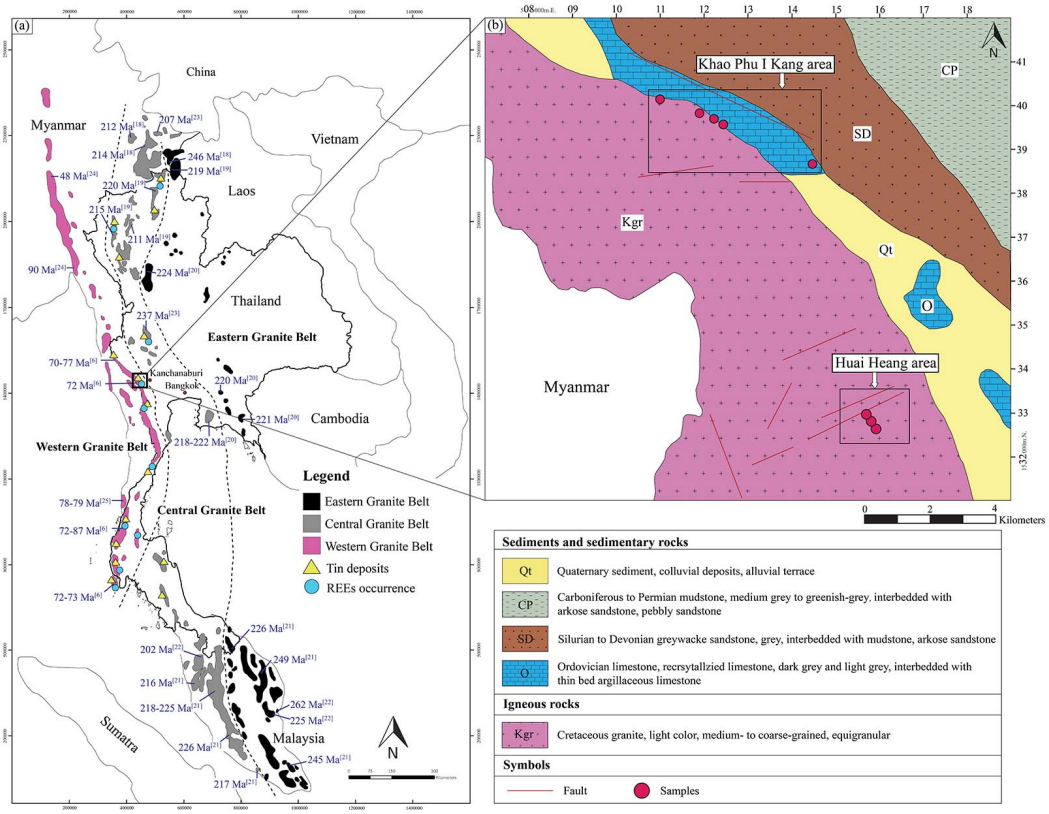

Fig. 1 (a) The Granite Belts in Southeast Asia separated into Eastern, Central, and Western Granite Belts. Tin deposits and REE occurrence are distributed along the Central and Western Granite Belts (modified after [4–6]). The ages of the granites were as reported [18–25]. (b) Geological map of the Ban Khao area consisting of limestone, sandstone, mudstone, and granite from Ordovician to Cretaceous age, showing the sampling locations at Huai Heang and Khao Phu I Kang areas (modified after [29–31]).

formed during the Late Permian to the Late Triassic through the subduction of oceanic plates beneath the Sibumasu and Indo-China microcontinents [6, 18–21]. The Central Granite Belt was formed in the Late Triassic to Middle Jurassic by the closure of the paleotethyan [16, 20–23]. The Western Granite Belt was formed during the Late Cretaceous to Middle Tertiary due to the collision between Sibumasu and Western Burma microcontinental plates [6, 24, 25]. Tin and tungsten deposits are dominantly associated with S-type granites of the Western Granite Belt with some deposits in the Central Granite Belt (Fig. 1(a)) [4–8].

The Western Granite Belt is distributed along the Thai-Myanmar border and crosses Chiang Rai, Kanchanaburi, Ratchaburi, Prachuab Khiri Khan, Ranong, Phang Nga, and Phuket Provinces. The granites in the belt in Chiang Rai, Kanchanaburi, Ratchaburi, Phang Nga, and Phuket Provinces are coarse- to medium-grained porphyritic and composed of leucogranite, biotite granite, and biotite-muscovite in the S-type granite, while some of the granites in Phuket (Khao Prathiu granite) and Phang Nga areas are I-type [9–11, 26, 27].

The geology of the Ban Khao area consists of limestone, sandstone, and mudstone from Ordovician to Permian, on which Cretaceous granite intruded as shown in Fig. 1(b) [28–30]. Ordovician rocks are composed of limestone, argillaceous limestone, sandy, and silty limestone which are formed bedded to massive, commonly interbedded with thin argillaceous bands containing cephalopods and crinoid stems. The Silurian to Devonian rocks are composed of sandstone interbedded with mudstone, sandstone, shale, and silt with tentaculites, while the Carboniferous to Permian rocks consist of laminated mudstone and lenticular fine-grained sandstone intercalated with sandstone [28–30]. Cretaceous granites of the Ban Kao area consist of porphyritic biotite granite, biotite-muscovite granite, and tourmaline-biotite granite [29–31]. These granites intruded into Ordovician limestone, sandstone, and mudstone, forming the hydrothermal alteration in the Huai Heang area and skarn in the Khao Phu I Kang area. The geology of the Huai Heang area consists of tourmaline-biotite granite and aplite which are hosted rocks of

quartz veins and the quartz-zinnwaldite-muscovite-cassiterite-tourmaline vein ranging from 5 to 20 cm thick. The tourmaline-biotite granite is altered and composed mainly of microcrystalline quartz, muscovite, zinnwaldite, and tourmaline. Rare earth minerals are formed in the tourmaline-biotite granite, aplite, quartz veins, and the quartz-zinnwaldite-muscovite-cassiterite-tourmaline vein. On the other hand, the geology of the Khao Phu I Kang skarn area consists of limestone, marble, tourmaline-biotite granite, garnet-pyroxene skarn, and quartz veins. Tourmaline-biotite granite intruded into the limestone, forming garnet-pyroxene skarn and quartz veins. The rare earth minerals are formed in the altered tourmaline-biotite granite.

MATERIALS AND METHODS

Twenty-six samples were collected from the Huai Heang area, consisting of tourmaline-biotite granite, pegmatite, aplite, quartz veins, and quartz-zinnwaldite-muscovite-cassiterite-tourmaline vein, and from the Khao Phu I Kang area consisting of limestone, marble, tourmaline-biotite granite, aplite, garnet-pyroxene skarn, and quartz veins (Fig. 1(b)). All the samples were prepared as polished thin sections using powder and diamond paste at the Department of Earth Sciences, Faculty of Science, Kasetsart University, Thailand. A Nikon polarized light microscope was used to observe petrographic characteristics. Mineralogy of 11 samples of tourmaline-biotite granite, pegmatite, aplite, quartz veins, and quartz-zinnwaldite-muscovite-cassiterite-tourmaline vein (Huai Heang area) and tourmaline-biotite granite, aplite, and garnet-pyroxene skarn (Khao Phu I Kang area) were analyzed using X-ray diffraction (Bruker D8 advance, Germany), and chemical compositions of the rare earth minerals were assessed using a scanning electron microscope with energy dispersive spectroscopy (SEM-EDS; model FEI Quanta 450 scanning electron microscope) at Kasetsart University. The conditions for SEM-EDS analysis were set at 15 kV.

RESULTS AND DISCUSSION

Petrography of granitic rocks at the Huai Heang area

The host rocks and veins in the Huai Heang area are composed of tourmaline-biotite granite, aplite, quartz veins, and quartz-zinnwaldite-muscovite-cassiterite-tourmaline vein.

The tourmaline-biotite granite has a phaneritic texture and is composed of quartz, plagioclase, K-feldspar, tourmaline, biotite, and muscovite with accessory zircon, apatite, ilmenite, cassiterite, monazite, and xenotime (Figs. 2(a) and 3(a)). The quartz shows an anhedral shape with a size ranging from 0.5 to 1.0 cm. Plagioclase is mainly replaced by sericite. The K-feldspar is euhedral with a perthitic texture

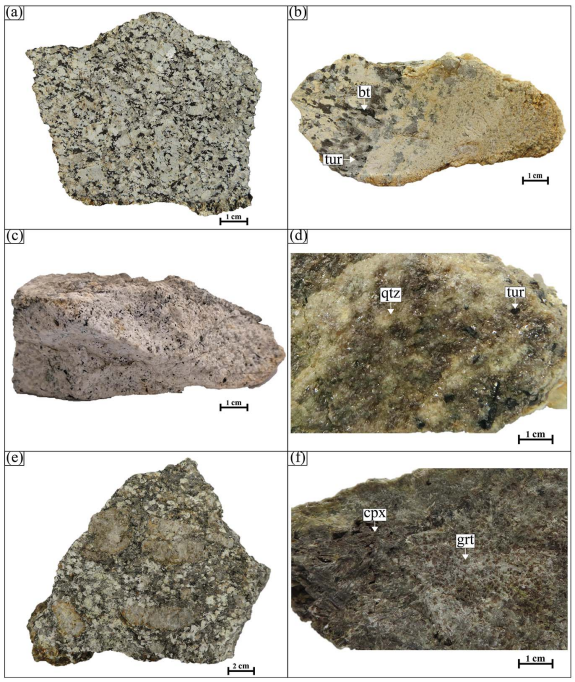

Fig. 2 Samples collected from the Ban Khao area. (a) Tourmaline-biotite granite collected from Huai Heang area. (b) Strongly altered tourmaline-biotite granite collected from the Huai Heang area. (c) Aplite collected from the Huai Heang area. (d) The quartz-zinnwaldite-muscovite-cassiterite-tourmaline vein sample collected from the Huai Heang area. (e) Tourmaline-biotite granite collected from the Kkao Phu I Kang area. (f) Garnet-pyroxene skarn collected from the Kkao Phu I Kang area. kfs: K-feldspar, bt: biotite, tur: tourmaline, qtz: quartz, grt: garnet, and cpx: clinopyroxene.

and size of 0.1–0.5 cm. Tourmaline mainly shows a euhedral shape with size ranging from 50 to 100 μm and accumulated texture around quartz. Biotite is characterized by brown color, lamellar texture, and pleochroic light brown to dark brown with zircon and apatite inclusions. Monazite shows subhedral to euhedral shape with size of 0.5–0.1 mm, while xenotime is subhedral with size of 0.1 to 0.5 mm. Monazite and xenotime are formed with tourmaline and biotite (Fig. 4(a,b)).

The altered tourmaline-biotite granite is cut by pegmatite dikes with approximately width of 30 cm in the NW-SE direction. The altered tourmaline-biotite granite shows moderate to strongly silicified alteration. The rock consists of microcrystalline quartz, zinnwaldite, biotite, muscovite, and tourmaline with rare earth minerals such as monazite and thorite (Fig. 2(b) and Fig. 3(b)). Zinnwaldite is characterized by a colorless lamellar texture with weak pleochroism from colorless to light brown (Fig. 3(c,d)). Monazite is a subhedral shape with size ranging from 10 to 50 μm

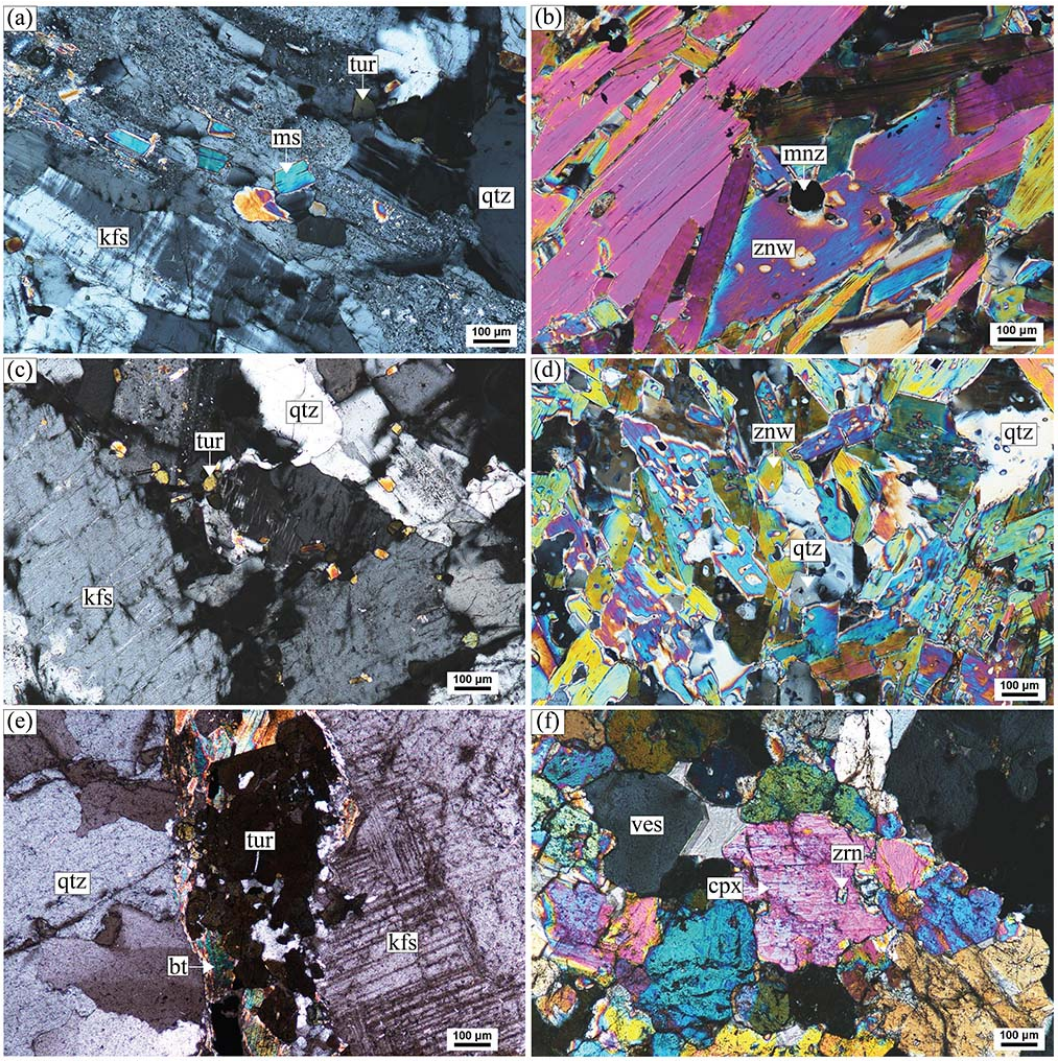

Fig. 3 Petrography of the samples under cross-polarization (XPL). (a) Tourmaline-biotite granite from the Huai Heang area consisting of quartz, K-feldspar, muscovite, and tourmaline. (b) Strongly altered tourmaline-biotite granite consisting of zinnwaldite and monazite. (c) Aplite from the Huai Heang area consisting of quartz, K-feldspar, and tourmaline. (d) The quartz-zinnwaldite-muscovite-cassiterite-tourmaline vein composed of microcrystalline quartz and zinnwaldite. (e) Tourmaline-biotite granite from the Khao Phu I Kang area consisting of quartz, K-feldspar, tourmaline, and biotite. (f) Garnet-pyroxene skarn consisting of clinopyroxene, garnet, and zircon. qtz: quartz, kfs: K-feldspar, ms: muscovite, tur: tourmaline, znw: zinnwaldite, mnz: monazite, bt: biotite, cpx: clinopyroxene, ves: vesuvianite, and zrn: zircon.

and forms accumulated crystal on biotite, while thorite is formed subhedral shape with size less than 50 µm (Fig. 4(c,d)).

The aplite is characterized by fine-grained, equigranular texture with a mineral grain size less than 1.0 mm and is composed of quartz, plagioclase, K-feldspar, tourmaline, and biotite with accessory zircon, apatite, and monazite (Fig. 2(c)). The quartz shows an anhedral and partly replaced by fine-grained tourmaline, while plagioclase is a subhedral to euhedral with size of 1.0 mm and partly replaced by sericite. K-feldspar shows a subhedral shape with a perthitic texture and size of 0.5–1.0 mm. Tourmaline is a subhedral to euhedral shape with size ranging from 0.1 to 0.3 mm, while biotite is lamellar shaped, showing brown, light brown to dark brown pleochroism. Monazite is characterized by a subhedral at size of 0.5 to 1.0 mm and occurs with tourmaline and biotite (Fig. 4(e)).

The veins in the Huai Haeng Sn deposit can be separated into quartz veins and quartz-zinnwaldite-muscovite-cassiterite-tourmaline vein. The quartz veins mainly comprise quartz with trace amounts of tourmaline and pyrite, while the quartz-zinnwaldite-

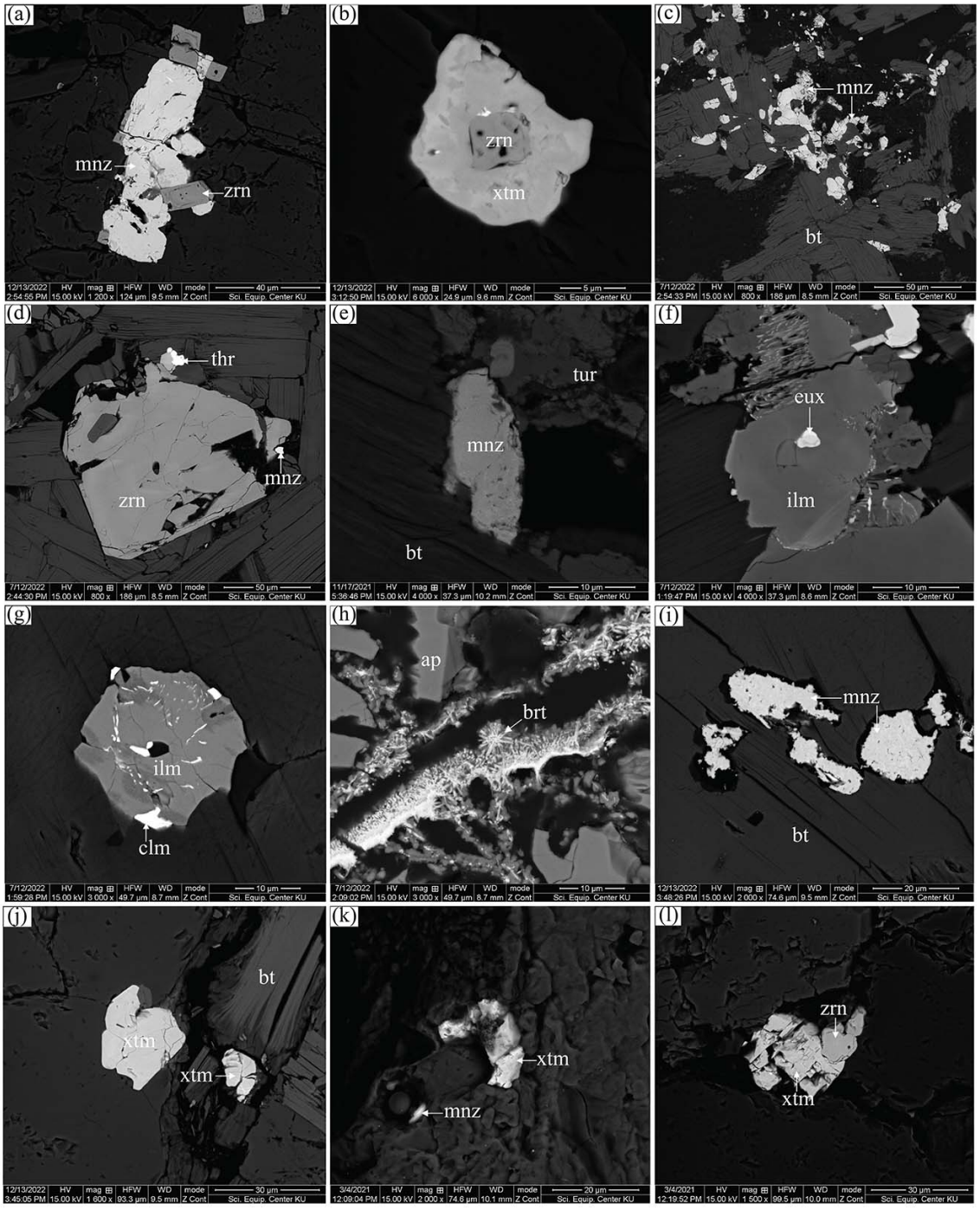

Fig. 4 Back-scattered electron images showing the texture of rare earth minerals in greisenization and skarn Sn deposits. (a) and (b) Monazite and xenotime formed with zircon in the tourmaline-biotite granite of greisenization Sn deposit. (c) Monazite showing accumulated texture with biotite in strongly altered tourmaline-biotite granite. (d) Monazite and thorite replaced at the edge of zircon crystals in strongly altered tourmaline-biotite granite. (e) Monazite formed with biotite and tourmaline in aplite of the greisenization Sn deposit. (f) Euxenite formed on ilmenite in the quartz-zinnwaldite-muscovite-cassiterite-tourmaline vein. (g) Columbite occurring as small inclusions in ilmenite in the quartz-zinnwaldite-muscovite-cassiterite-tourmaline vein. (h) Britholite formed as an aggregate texture in apatite fractures of the quartz-zinnwaldite-muscovite-cassiterite-tourmaline vein. (i) and (j) Monazite and xenotime formed with biotite in the tourmaline-biotite granite skarn Sn deposit. (k) and (l) Monazite and xenotime found in aplite of the skarn Sn deposits. mnz: monazite, zrn: zircon, xtm: xenotime, bt: biotite, thr: thorite, tur tourmaline, eux: euxenite, ilm: ilmenite, clm: columbite, brt: britholite, and ap: apatite.

muscovite-cassiterite-tourmaline vein contains abundant quartz, zinnwaldite, and muscovite with small amounts of tourmaline, cassiterite, zircon, apatite, ilmenite, cassiterite, euxenite, columbite, and britholite (Fig. 2(d), Fig. 3(d), and Fig. 4(f–h)).

The occurrence of rare earth minerals in the rocks and veins can be separated into disseminated monazite and xenotime in the unaltered rocks and thorite, monazite, euxenite, columbite, and britholite in the strongly altered rocks and veins. Columbite is a typical product of the hydrothermal alteration in alkaline granite during the later stage of alteration formed by hydrothermal fluid [32–34]. Various rare earth minerals in the strongly altered rocks and veins indicate that the hydrothermal fluid contained the rare earth elements which interacted with the rocks and precipitated in the veins as the greisenization process [34, 35].

Petrography of granitic rocks and skarn at the Khao Phu I Kang area

The host rocks in the Khao Phu I Kang Sn deposit are tourmaline-biotite granite, aplite, and garnet-pyroxene skarn.

Tourmaline-biotite granite is characterized by porphyritic texture of K-feldspar (1.0 to 2.0 cm) and is composed of quartz, K-feldspar, plagioclase, and biotite with accessory tourmaline, zircon, apatite, ilmenite, monazite, and xenotime (Fig. 2(e) and Fig. 3(e)). The quartz shows an anhedral shape which is partly replaced by biotite. K-feldspar is a subhedral shape (0.1 to 0.5 mm) with tartan twinning. Biotite is brown and lamellar shaped with size ranging from 0.1 to 0.5 mm and exhibits strong pleochroism (light brown to dark brown). Zircon shows euhedral crystals with size less than 100 µm and forms inclusions on biotite with ilmenite and apatite. Monazite and xenotime are characterized by subhedral to euhedral shape with size ranging from 0.5 to 1.0 mm which are formed with biotite (Fig. 4(i,j)).

Aplite is characterized by fine-grained size (< 1 mm) and equigranular texture and consists of quartz, plagioclase, K-feldspar, biotite, and tourmaline with accessory zircon, monazite, and xenotime. The quartz shows anhedral shape, while plagioclase and K-feldspar show a subhedral to euhedral shape. Biotite is brown and lamellar shaped. The tourmaline is formed as euhedral shape with size of 0.5 mm, while monazite is a subhedral shape (0.3 to 0.5 mm), and xenotime is a subhedral to euhedral which is formed with zircon (Fig. 4(k,l)).

The Khao Phu I Kang area is formed as skarn by tourmaline-biotite granite intruding into limestone. A garnet-pyroxene zone occurs between the tourmaline-biotite granite and limestone. This garnet-pyroxene skarn consists of clinopyroxene, garnet, vesuvianite, and epidote (Fig. 2(f) and Fig. 3(f)). The vesuvianite is an anhedral to subhedral shape and overprinted by fine- to medium- grained (0.5 to 1.0 mm), subhedral to euhedral shape. It is formed with garnet and replaced by epidote. Epidote replaces clinopyroxene and vesuvianite. Cassiterite is also formed in the garnet-pyroxene zone with zircon, pyrite, and sphalerite. However, monazite and xenotime are not present in this zone.

Rare earth minerals in greisenization and skarn Sn deposits

Rare earth minerals in greisenization and skarn Sn deposits can be classified into monazite, xenotime, thorite, euxenite, columbite, and britholite based on crystal shape and chemical composition. Monazite and xenotime are formed as accessory minerals in the tourmaline-biotite granite and aplite, while thorite, euxenite, columbite, and britholite are formed in the strongly altered tourmaline-biotite granite and quartz-zinnwaldite-muscovite-cassiterite-tourmaline vein, as shown in Fig. 4.

Monazite and xenotime are formed disseminated in tourmaline-biotite granite and aplite in the Huai Heang Sn deposit and Khao Phu I Keang skarn. Monazite is characterized by subhedral to euhedral crystals with size of 0.5 to 1.0 mm (Fig. 4(a,e,i,k)) and composed of 25.4–30.5 wt.% Ce_2O_3, 8.9–22.3 wt.% La_2O_3, 5.2–19.0 wt.% Nd_2O_3, 1.4–11.1 wt.% Y_2O_3, 0.6–2.4 wt.% Gd_2O_3, and 0.1–1.2 wt.% Dy_2O_3. Xenotime is formed as subhedral to euhedral shape with size of 0.1 to 0.5 mm (Fig. 4(b,j,l)) and consists of 43.3–55.4 wt.% Y_2O_3, 1.0–8.6 wt.% Dy_2O_3, and 0.9–2.7 wt.% Gd_2O_3, analyzed using a scanning electron microprobe and energy dispersive (SEM-EDS) analysis (Table 1).

Thorite and monazite are formed in the strongly altered tourmaline-biotite granite, while euxenite, columbite, and britholite occur in the quartz-zinnwaldite-muscovite-cassiterite-tourmaline vein. Monazite shows irregular to anhedral crystals, ranging from 10 to 50 µm and accumulated in strongly altered tourmaline-biotite granite (Fig. 4(c)). Monazite is composed mainly of 27.1–28.5 wt.% Ce_2O_3, 12.5–14.5 wt.% La_2O_3, and 8.4–10.0 wt.% Nd_2O_3. Thorite is characterized by subhedral shape with size of less than 50 µm and formed at the edge of zircon crystals containing 4.5 wt.% Y_2O_3 (Fig. 4(d)). Euxenite and columbite are formed as small inclusions in ilmenite (4–10 µm) (Fig. 4(f,g)). Euxenite is composed of 8.8–9.7 wt.% Y_2O_3, while columbite consists of 1.2–1.6 wt.% Y_2O_3. In addition, the britholite ($(REECa)_5(SiO_4,PO_4)_3(OH,F)$) is formed in apatite fractures in the quartz-zinnwaldite-muscovite-cassiterite-tourmaline vein (Fig. 4(h)) which contains 11.4–13.1 wt.% La_2O_3, 11.4–12.0 wt.% Nd_2O_3, 6.4–7.2 wt.% Ce_2O_3, 1.8–3.1 wt.% Y_2O_3, 1.4–2.0 wt.% Gd_2O_3, and 1.0–1.3 wt.% Dy_2O_3 (Fig. 4(b) and

Table 1 Chemical compositions of monazite and xenotime in aplite and tourmaline-biotite granite greisenization and skarn Sn deposits analyzed by a scanning electron microprobe and energy dispersive (SEM-EDS) analysis.

Greisenization Sn Deposit										
Rock	Aplite				Tourmaline-biotite granite					
Sample no.	mnz-1	mnz-2	mnz-3	mnz-4	mnz-5	mnz-6	mnz-7	mnz-8	xtm-1	xtm-2
P_2O_5	35.45	34.92	36.30	32.54	32.79	30.86	35.54	34.69	40.28	39.98
Y_2O_3	1.93	1.92	1.38	2.26	3.45	3.42	4.87	4.13	48.70	43.34
La_2O_3	12.97	13.11	10.98	10.44	14.81	13.65	11.50	12.22	0.00	0.26
Ce_2O_3	26.24	26.00	26.69	26.44	29.86	27.22	24.56	26.89	0.08	0.44
Nd_2O_3	8.43	8.20	8.83	8.32	9.07	7.78	7.97	8.56	0.40	0.16
Gd_2O_3	0.65	0.69	0.73	1.71	1.19	0.66	0.81	0.74	1.56	1.53
Dy_2O_3	–	0.22	–	–	–	0.12	0.53	0.11	4.18	4.86
ThO_2	12.20	13.80	13.50	14.20	8.65	15.60	12.50	12.27	0.62	1.27
UO_3	0.81	0.20	0.40	2.40	0.18	0.68	1.72	0.39	4.00	7.40
Total	98.67	99.06	98.81	98.29	100.00	99.99	100.00	100.00	99.82	99.25
atoms per formula unit (apfu) on the basis of 40										
P	1.10	1.09	1.12	1.06	1.05	1.02	1.09	1.08	1.05	1.06
Y	0.04	0.04	0.03	0.05	0.07	0.07	0.09	0.08	0.80	0.72
La	0.18	0.18	0.15	0.15	0.21	0.20	0.15	0.17	0.00	0.00
Ce	0.35	0.35	0.35	0.37	0.41	0.39	0.33	0.36	0.00	0.01
Nd	0.11	0.11	0.11	0.11	0.12	0.11	0.10	0.11	0.00	0.00
Gd	0.01	0.01	0.01	0.02	0.01	0.01	0.01	0.01	0.02	0.02
Dy	0.00	0.00	0.00	0.00	0.00	0.00	0.01	0.00	0.04	0.05
Th	0.10	0.12	0.11	0.12	0.07	0.14	0.10	0.10	0.00	0.01
U	0.01	0.00	0.00	0.02	0.00	0.01	0.01	0.00	0.03	0.05
Skarn Sn deposit										
Rock	Aplite		Tourmaline-biotite granite		Aplite		Tourmaline-biotite granite			
Sample no.	mnz-9	mnz-10	mnz-11	mnz-12	xtm-3	xtm-4	xtm-5	xtm-6	xtm-7	xtm-8
P_2O_5	41.14	30.38	37.85	37.43	40.06	40.59	42.32	40.85	41.54	41.91
Y_2O_3	2.44	8.64	11.17	9.03	49.19	50.99	53.23	55.43	54.05	53.30
La_2O_3	15.15	22.33	19.51	19.25	0.00	–	–	–	–	–
Ce_2O_3	30.55	18.85	4.37	5.36	0.00	–	–	–	–	–
Nd_2O_3	9.66	5.19	19.09	18.57	0.00	–	–	–	0.07	–
Gd_2O_3	0.80	–	2.15	2.45	1.98	2.75	1.42	2.64	0.91	0.89
Dy_2O_3	0.21	–	1.20	0.01	8.63	5.67	3.03	1.07	2.87	3.00
ThO_2	0.00	14.61	–	2.90	0.00	–	–	–	–	–
UO_3	–	–	4.66	5.00	0.00	–	–	–	0.56	0.90
Total	99.94	100.00	100.00	100.00	99.86	100.00	100.00	99.99	100.00	100.00
atoms per formula unit (apfu) on the basis of 40										
P	1.16	1.00	1.10	1.10	1.05	1.05	1.07	1.04	1.06	1.06
Y	0.04	0.18	0.20	0.17	0.81	0.83	0.84	0.89	0.86	0.85
La	0.19	0.32	0.25	0.25	0.00	0.00	0.00	0.00	0.00	0.00
Ce	0.37	0.27	0.05	0.07	0.00	0.00	0.00	0.00	0.00	0.00
Nd	0.12	0.07	0.23	0.23	0.00	0.00	0.00	0.00	0.00	0.00
Gd	0.01	0.00	0.02	0.03	0.02	0.03	0.01	0.03	0.01	0.01
Dy	0.00	0.00	0.01	0.00	0.09	0.06	0.03	0.01	0.03	0.03
Th	0.00	0.13	0.00	0.02	0.00	0.00	0.00	0.00	0.00	0.00
U	0.00	0.00	0.03	0.04	0.00	0.00	0.00	0.00	0.00	0.01

Abbreviations: mnz: monazite, xtm: xenotime.

Table 2). The occurrence of britholite is related to hydrothermal solutions in the strong alteration and vein.

Monazite in the granite was reacted with the fluid at the temperature around 200 °C of the greisenization alteration to form thorite ($Th(SiO_4)$) with monazite related to hydrothermal alteration [35–37]. The chemical composition of monazite suggests that thorite was formed by REE^{3+} and P^{5+} to produce $(Y, Gd, Dy)^{3+}$, $(Th, U)^{4+}$, and Si^{4+} [37]. The presence of euxenite and columbite with ilmenite in the quartz-zinnwaldite-muscovite-cassiterite-tourmaline vein indicates that HREEs such as Y_2O_3 of euxenite and columbite were formed by exsolution from the hydrothermal fluid

Table 2 Chemical compositions of monazite, thorite, euxenite, columbite, and britholite in strongly altered tourmaline-biotite granite and quartz-zinnwaldite-muscovite-cassiterite-tourmaline vein of greisenization Sn deposit using a scanning electron microprobe and energy dispersive (SEM-EDS) analysis.

Greisenization Sn deposit										
Rock	Strongly altered tourmaline-biotite granite					quartz-zinnwaldite-muscovite-cassiterite-tourmaline vein				
Sample no.	mnz-1	mnz-2	mnz-3	mnz-4	thr	eux-1	eux-2	clm-1	clm-2	clm-3
MgO	–	–	–	–	–	–	–	0.53	–	0.14
Al_2O_3	–	–	–	–	–	3.14	3.37	4.41	3.83	2.66
SiO_2	–	–	–	–	17.64	8.38	10.45	9.42	7.67	6.84
K_2O	–	–	–	–	–	0.97	–	1.18	1.28	1.20
P_2O_5	34.15	33.29	32.87	37.39	11.79	–	–	–	–	
CaO	–	–	–	–	2.24	0.25	–	0.40	–	–
TiO_2	–	–	–	–	–	38.43	45.87	2.96	10.67	11.03
MnO	–	–	–	–	–	–	–	7.43	7.96	10.74
FeO	–	–	–	–	2.46	1.66	2.17	7.88	6.42	11.70
Y_2O_3	–	–	–	–	4.82	9.69	8.80	1.63	–	1.28
Nb_2O_5	–	–	–	–	–	18.27	18.24	43.10	43.48	41.07
La_2O_3	14.36	13.40	15.59	15.85	–	–	–	–	–	–
Ce_2O_3	29.06	28.99	30.45	31.99	–	–	–	–	–	–
Pr_2O_3	2.15	2.77	2.21	–	–	–	–	–	–	–
Nd_2O_3	9.02	10.72	9.03	10.35	–	–	–	–	–	–
Sm_2O_3	0.54	1.01	0.55	1.14	–	–	–	–	–	–
Eu_2O_3	0.22	0.62	0.44	0.49	–	–	–	–	–	–
Gd_2O_3	1.35	1.18	0.86	0.66	0.46	–	–	–	–	–
Dy_2O_3	0.36	0.20	0.49	0.10	0.98	–	–	–	–	–
SnO_2	–	–	–	–	–	1.10	–	–	–	–
Ta_2O_5	–	–	–	–	–	1.54	0.98	12.22	11.46	7.80
ThO_2	8.55	7.84	6.96	1.92	47.80	–	–	–	–	–
UO_3	–	–	–	–	11.10	16.56	10.13	–	–	–
WO_3	–	–	–	–	–	–	–	8.84	7.22	5.55
Total	99.77	100.01	99.45	99.89	99.30	99.99	100.01	100.00	99.99	100.01
atoms per formula unit (apfu) on the basis of 40* and 60**										
Mg	–	–	–	–	–	0.00	0.00	0.10	0.00	0.02
Al	–	–	–	–	–	0.25	0.23	0.66	0.53	0.34
Si	0.00	0.00	0.00	0.00	0.72	0.56	0.60	1.20	0.90	0.73
K	–	–	–	–	–	0.08	0.00	0.19	0.19	0.16
P	1.08	1.06	1.06	1.12	0.41	–	–	–	–	–
Ca	0.00	0.00	0.00	0.00	0.10	0.02	0.00	0.05	0.00	0.00
Ti	–	–	–	–	–	1.92	1.98	0.28	0.94	0.89
Mn	–	–	–	–	–	0.00	0.00	0.80	0.79	0.98
Fe	0.00	0.00	0.00	0.00	0.08	0.09	0.10	0.84	0.63	1.05
Y	0.00	0.00	0.00	0.00	0.10	0.34	0.27	0.11	0.00	0.07
Nb	–	–	–	–	–	0.55	0.47	2.47	2.31	1.99
La	0.20	0.19	0.22	0.21	0.00	–	–	–	–	–
Ce	0.40	0.40	0.42	0.41	0.00	–	–	–	–	–
Pr	0.03	0.04	0.03	0.00	0.00	–	–	–	–	–
Nd	0.12	0.14	0.12	0.13	0.00	–	–	–	–	–
Sm	0.01	0.01	0.01	0.01	0.00	–	–	–	–	–
Eu	0.00	0.01	0.01	0.01	0.00	–	–	–	–	–
Gd	0.02	0.01	0.01	0.01	0.01	–	–	–	–	–
Dy	0.00	0.00	0.01	0.00	0.01	–	–	–	–	–
Sn	–	–	–	–	–	0.03	0.00	0.00	0.00	0.00
Ta	–	–	–	–	–	0.03	0.02	0.42	0.37	0.23
Th	0.07	0.07	0.06	0.02	0.44	–	–	–	–	–
U	0.00	0.00	0.00	0.00	0.10	0.23	0.12	0.00	0.00	0.00
W	–	–	–	–	–	0.00	0.00	0.29	0.22	0.15

Abbreviations: mnz: monazite, thr: thorite, eux: euxenite, clm: columbite. * calculated atoms per formula unit (apfu) on the basis of 40 for monazite and thorite; ** calculated atoms per formula unit (apfu) on the basis of 60 for euxenite and columbite.

Table 3 Chemical compositions of britholite in the quartz-zinnwaldite-muscovite-cassiterite-tourmaline vein of greisenization Sn deposit using a scanning electron microprobe and energy dispersive (SEM-EDS) analysis.

quartz-zinnwaldite-muscovite-cassiterite-tourmaline vein			
Sample no.	brt-1	brt-2	brt-3
SiO_2	7.72	14.72	9.14
P_2O_5	33.43	33.54	33.77
CaO	5.90	4.72	5.83
Y_2O_3	3.06	2.48	1.88
La_2O_3	11.45	13.06	12.80
Ce_2O_3	7.13	6.39	7.22
Pr_2O_3	3.30	3.40	3.34
Nd_2O_3	11.45	12.90	12.04
Pm_2O_3	0.35	–	–
Sm_2O_3	2.89	2.13	2.32
Eu_2O_3	1.17	0.17	0.29
Gd_2O_3	2.03	1.67	1.45
Ho_2O_3	1.11	1.29	1.03
Dy_2O_3	–	0.27	0.12
Er_2O_3	–	0.54	0.42
Yb_2O_3	0.90	0.59	0.46
Lu_2O_3	–	0.17	0.15
ThO_2	7.69	1.87	7.22
Total	99.58	99.91	99.48
atoms per formula unit (apfu) on the basis of 12O			
Si	0.77	1.35	0.89
P	2.81	2.60	2.78
Ca	0.63	0.46	0.61
Y	0.16	0.12	0.10
La	0.42	0.44	0.46
Ce	0.26	0.21	0.26
Pr	0.12	0.11	0.12
Nd	0.41	0.42	0.42
Pm	0.01	0.00	0.00
Sm	0.10	0.07	0.08
Eu	0.04	0.01	0.01
Gd	0.07	0.05	0.05
Dy	0.04	0.04	0.03
Ho	0.00	0.01	0.00
Er	0.00	0.02	0.01
Yb	0.03	0.02	0.01
Lu	0.00	0.00	0.00
Th	0.17	0.04	0.16

Abbreviation: brt: britholite.

in an exsolution [33, 38]. Ilmenite in the quartz-zinnwaldite-muscovite-cassiterite-tourmaline vein occurs with columbite formed in fracture as shown in the Fig. 4(g), in which the columbite is related to the hydrothermal altered alkaline granite [32–34]. Britholite in apatite fractures is formed with calcium, silicon, and fluorine. The element composition of apatite ($Ca_5(PO_4)_3(OH,F,Cl)$) such as calcium, phosphorus, and silicon is reacted by the hydrothermal fluid and forms britholite in the apatite crystal fractures [39, 40]. The hydrothermal fluid interacts with the tourmaline-biotite granite and aplite to form various rare earth minerals such as thorite, euxenite, columbite, and britholite by greisenization at a temperature of around 200 °C.

CONCLUSION

Tourmaline-biotite granite and aplite are the host rocks of the quartz-zinnwaldite-muscovite-cassiterite-tourmaline vein containing euxenite, thorite, columbite, britholite, and quartz veins, which are formed by greisenization of hydrothermal alterations. Rare earth minerals such as monazite and xenotime occur as accessories in the tourmaline-biotite granite and aplite. Thorite and irregular monazite are formed mainly in the strongly altered tourmaline-biotite granite, while columbite, euxenite, and britholite are mainly formed in the quartz-zinnwaldite-muscovite-cassiterite-tourmaline vein.

Acknowledgements: This research is supported in part by the Graduate Program Scholarship from the Graduate School, Kasetsart University. In addition, we gratefully thank Nuclear Technology Research and Development Center, Thailand Institute of Nuclear Technology and Department of Earth Sciences, Faculty of Science, Kasetsart University for their equipment, valuable comments, and advice. The authors would like to thank the three reviewers for their careful reading of our manuscript and many constructive comments and suggestions.

REFERENCES

1. Goonan TG (2011) *Rare Earth Elements – End Use and Recyclability: U.S. Geological Survey Scientific Investigations Report 2011-5094*, U.S. Geological Survey, Reston, Virginia, USA.
2. Van Gosan BS, Verplanck PL, Seal II RR, Long KR, Gambogi J (2017) Rare-earth elements. In: Schulz KJ, DeYoung JH, Seal II RR, Bradley DC (eds) *Critical Mineral Resources of the United States-Economic and Environmental Geology and Prospects for Future Supply*, U.S. Geological Survey, USA, pp 1–31.
3. Kanazawa Y, Kamitani M (2006) Rare earth minerals and resources in the world. *J Alloys Compd* **408–412**, 1139–1343.
4. Cobbing EJ, Mallick DIJ, Pitfield PEJ, Teoh LH (1986) The granites of the Southeast Asian Tin Belt. *J Geol Soc London* **143**, 537–550.
5. Schwartz MO, Rajah SS, Askury AK, Putthapiban P, Djaswadi S (1995) The Southeast Asian Tin Belt. *Earth-Sci Rev* **38**, 95–293.
6. Charusiri P, Clark AH, Farrar E, Archibald D, Charusiri B (1993) Granite belts in Thailand: evidence from the $^{40}Ar/^{39}Ar$ geochronological and geological syntheses. *J Asian Earth Sci* **8**, 127–136.
7. Pangrassami T, Sanguansai P (1991) An overview on rare earth mineral resources/reserves of active tin mines in Thailand. *Mater Sci Forum* **70–72**, 557–576.
8. Nakapudungrat S, Putthapiban P (1992) Granites and associated mineralization in Thailand. In: *National Conference on Geological Resources of Thailand: Potential for Future Development*, Bangkok, pp 153–166.
9. Chualaowanich T, Chamraswai U, Watcharamai T, Punyawai W (2011) *Exploration and Assessment of Tin and Lead, Kanchanaburi Province*, Department of Mineral Resources, Bangkok, Thailand.

10. Mahawat C (1984) The geological characteristics of the Pilok Sn-W-Mo deposits, west Thailand. In: *International Symposium on the Geology of Tin Deposits*, China, pp 95–108.
11. Linnen R, Williams-Jones AE (1995) Genesis of a magmatic metamorphic hydrothermal system: The Sn-W polymetallic deposits at Pilok, Thailand. *Econ Geol* **90**, 1148–1166.
12. Stemprok M (1987) Greisenization (a review). *Geol Rundsch* **76**, 169–175.
13. Lamarao CN, Pinho SCC, Paiva ALJ, Galarza MA (2012) Mineralogy and geochemistry of the Paleoproterozoic, tin-mineralized Bom Jardim granite of the Velho Guilherme Suite, eastern Amazonian craton. *J South Am Earth Sci* **38**, 159–173.
14. Chen J, Halls C, Stanley CJ (1992) Rare earth element contents and patterns in major skarn minerals from Shizhuyuan W, Sn, Bi and Mo deposit, South China. *Geochem J* **26**, 147–158.
15. Fitros M, Tombros SF, Kokkalas S, Kilias SP, Perraki M, Skliros V, Simos XC, Papaspyropoulos K, et al (2020) REE-enriched skarns in collisional settings: The example of Xanthi's Fe-skarn, Rhodope Metallogenetic Massif, Northern Greece. *Lithos* **370–371**.
16. Tukpho T, Fanka A (2021) Petrology and geochemistry of granitic rocks in Dan Chang area, Suphan Buri Province, Central Thailand: Implication for petrogenesis. *ScienceAsia* **47**, 609–617.
17. Jiang H, Zhao KD, Jiang SY, Li WQ, Zaw K, Zhang D (2021) Late Triassic post-collisional high-K two-mica granites in Peninsular Thailand, SE Asia: Petrogenesis and Sn mineralization potential. *Lithos* **436–437**, 1–17.
18. Cong F, Wu FY, Li WC, Wang JG, Hu FY, He DF, Ji WQ, Lin W, et al (2021) Petrogenesis of the main range and eastern province granites in eastern Myanmar: New insights from zircon U-Pb ages and Sr-Nd isotopes. *Lithos* **382–383**.
19. Wang Y, He H, Cawood PA, Srithai B, Feng Q, Fan W, Zhang Y, Qian X (2016) Geochronological, elemental and Sr-Nd-Hf-O isotopic constraints on the petrogenesis of the Triassic post-collisional granitic rocks in NW Thailand and its Paleotethyan implications. *Lithos* **266–267**, 264–286.
20. Qian X, Feng Q, Wang Y, Zhao T, Zi JW, Udchachon M, Wang Y (2017) Late Triassic post-collisional granites related to Paleotethyan evolution in SE Thailand: Geochronological and geochemical constraints. *Lithos* **286–287**, 440–453.
21. Ng SWP, Whitehouse MJ, Searle MP, Robb LJ, Ghani AA, Chung SL, Oliver GJH, Sone M, et al (2015) Petrogenesis of Malaysian granitoids in the Southeast Asian tin belt: Part 2. U-Pb zircon geochronology and tectonic model. *Geol Soc Am Bull* **127**, 1238–1258.
22. Liu L, Hu RZ, Zhong H, Yang JH, Kang LF, Zhang XC, Fu YZ, Mao W, et al (2020) Petrogenesis of multistage S-type granites from the Malay Peninsula in the Southeast Asian tin belt and their relationship to Tethyan evolution. *Gondwana Res* **84**, 20–37.
23. Nakapadungrat S (1982) Geochoronology and Geochemistry of The Thong-Lang Granite Complex, Central Thailand. *PhD Dissertation*, University of London.
24. Myint AZ, Zaw K, Swe YM, Yonezu K, Cai Y, Manaka T, Watanabe K (2017) Geochemistry and geochronology of granites hosting the Mawchi Sn-W deposit, Myanmar: implications for tectonic setting and emplacement. In:@ Barber AJ, Zaw K, Crow MJ (eds) *Myanmar: Geology, Resources and Tectonics*, The Geological Society of London, London, pp 385–400.
25. Oo ZM, Zaw K, Belousov I, Putthipiban P, Makoundi C (2023) Tectonic and metallogenic implications of W-Sn related granitoid rocks in the Kawthaung-Bankachon area, southernmost part of Myanmar: Constraints from petrology, geochemistry, and U-Pb zircon geochronology. *Geosyst Geoenviron* **2**, 100188.
26. Charusiri P, Pongsapich W, Vedchakanchana S (1986) Petrological and geochemical studies of granites of Kathu Plutons of Phuket Island, Southern Thailand. *Geol Soc Malaysia Bulletin* **19**, 261–280.
27. Phountong K, Salam A, Manaka T (2020) Petrochemistry of granite from Takua Pit Thong area, Ratchaburi, Thailand. *Bull Earth Sci Thailand* **12**, 15–29.
28. Department of Mineral Resources (2008) *Geology of Kanchanaburi*, Department of Mineral Resources, Bangkok, Thailand.
29. Chualaowanich T, Watcharamai T, Punyawai W, Insri T (2012) *Exploration and Assessment of Heavy Minerals – Rare Earth Element, Kanchanaburi Province*, Department of Mineral Resources, Bangkok, Thailand.
30. Watcharamai T (2018) *Distribution of Rare Earth Elements in Granite at Kanchanaburi and Uthai Thani Provinces*, Department of Mineral Resources, Bangkok, Thailand.
31. Sukbunjong B, Tangwattananukul L, Nuchdang S, Buranrom S, Wongkham W (2022) Occurrence of monazite and xenotime around Jarin tin deposit in Kanchanaburi Province, Thailand. In: *6th GEOINDO 2022*, Khon Kaen, Thailand, pp 65–72.
32. Uher P, Ondrejka M, Konečny P (2009) Magmatic and post-magmatic YREE-Th phosphate, silicate and Nb-Ta-Y-REE oxide minerals in A-type metagranite: an example from the Turčok massif, the Western Carpathians, Slovakia. *Minaral Mag* **73**, 1009–1025.
33. Macdonald R, Bagiński B, Martashov P, Zozulya D, Dzierżanowski P, Jokubauskas P (2015) Hydrothermal alteration of a chevkinite-group mineral to a bastnäsite-(Ce)-ilmenite- columbite-(Fe) assemblage: interaction with a F-, CO_2-rich fluid. *Miner Petrol* **109**, 659–678.
34. Siachoque A, Garcia R, Vlach SRF (2020) Occurrence and composition of columbite-(Fe) in the reduced A-Type Desemborque Pluton, Graciosa Province (S-SE Brazil). *Minerals* **10**, 1–16.
35. Tillberg M, Maskenskaya OM, Drake H, Hogmalm JH, Broman C, Fallick AE, Astrom ME (2019) Fractionation of rare earth elements in greisen and hydrothermal veins related to A-type magmatism. *Geofluids* **2019**, 1–20.
36. Poitrasson F, Chenery S, Bland D (1996) Contrasted monazite hydrothermal alteration mechanisms and their geochemical implications. *Earth Planet Sci Lett* **145**, 79–96.
37. LeBoutillier NG, Shail RK, Jewson C (2003) Monazite in polymetallic chlorite-(tourmaline)-quartz-(fluorite)-cassiteritesulphide lodes and its potential for constraining the chronology of magmatic hydrothermal mineralisation in Cornwall. *Geoscience in south-west England* **10**, 403–409.
38. Duran CJ, Seydoux-Guillaume AM, Bingen B, Gouy

S, Parseval PD, Ingrin J, Guillaume D (2016) Fluid-mediated alteration of (Y,REE,U,Th)-(Nb,Ta,Ti) oxide minerals in granitic pegmatite from the Evje-Iveland district, southern Norway. *Miner Petrol* **110**, 581–599.

39. Lorrenz M, Altenberger U, Trumbull RB, Lira R, Luchi MLD, Gunter C, Eidner S (2019) Chemical and textural relations of britholite- and apatite-group minerals from hydrothermal REE mineralization at the Rodeo de los Molles deposit, Central Argentina. *Am Mineral* **104**, 1840–1850.

40. Uher P, Ondrejka M, Bačík P, Broska I, Konečný P (2015) Britholite, monazite, REE carbonates, and calcite: Products of hydrothermal alteration of allanite and apatite in A-type granite from Stupné, Western Carpathians, Slovakia. *Lithos* **236–237**, 212–225.